

Structural investigation of amorphous materials at high pressures using the diamond anvil cell

Guoyin Shen,^{a)} Vitali B. Prakapenka, Mark L. Rivers,^{b)} and Stephen R. Sutton^{b)}
Consortium for Advanced Radiation Sources, University of Chicago, Chicago, Illinois 60637

(Received 9 December 2002; accepted 17 March 2003)

A modified diamond anvil cell (DAC) is used for structural studies of amorphous materials at high pressures using a monochromatic synchrotron x-ray beam. The DAC modification includes (1) the use of x-ray transparent seats for a large angular opening for x-ray scattering, and (2) the introduction of a boron gasket insert to increase the sample thickness and to minimize the gasket-hole deformation. A procedure for absorption correction and background subtraction in DAC experiments is described, together with an optimization process for obtaining accurate data of the structure factor and the corresponding pair distribution function. Data for amorphous iron at 67 GPa are presented for demonstration. It is shown that quantitative structural data can be determined for amorphous materials at very high pressures using the DAC. The apparatus should be also useful for structural studies of liquids at high pressures. © 2003 American Institute of Physics.
[DOI: 10.1063/1.1574394]

I. INTRODUCTION

The study of the structure of noncrystalline materials at high pressure has been a long-standing goal in high-pressure research. It is of great importance in materials science and geophysics, because information on the structure of liquids or amorphous materials provides a basis for investigating numerous macroscopic physical properties such as viscosity and self-diffusion,¹ electrical resistivity,² compressibility,³ and thermal expansion.⁴ There are growing numbers of structural studies of noncrystalline materials at high pressure and high temperature. Novel and interesting phenomena have been reported, e.g., the observation of first-order phase transitions in liquid phosphorus⁵ and liquid GeSe₂.⁶

Liquids and amorphous materials exhibit weak diffuse x-ray scattering, which leads to major difficulties in high-pressure experiments due to the small sample volume and the relatively large background scattering from sample containers in high-pressure instruments. With the development of synchrotron sources, significant progress has been made in structural studies of noncrystalline materials at high pressures. The brilliant synchrotron beam makes it possible to measure the weak diffuse scattering from small high-pressure samples. To reduce the background signal, energy dispersive scattering (EDS) has often been used, with careful spatial collimation of the scattered signals.^{5,7} The EDS method involves data collection at several 2θ angles and intensity normalization to the x-ray source spectrum, which extends the measurement time and could degrade the accuracy in intensity. Angle dispersive scattering (ADS) has the intrinsic advantage of obtaining accurate intensity information, and has been applied in large volume presses with a

multislit system for spatial collimation.⁸ The combination of an area detector with collimation slits results in accurate scattering intensities and an effective reduction of the background signal, making it an effective tool for studying the structure of noncrystalline materials at extreme conditions with large volume presses. It is desirable to have a similar multichannel slit system for spatial collimation in experiments with the diamond anvil cell (DAC), with which much higher pressures can be reached. On the other hand, because the anvil materials in the DAC are single crystals, it is found to be possible, even without spatial collimation, to measure the scattering from noncrystalline samples with a proper background subtraction. Eggert *et al.*⁹ used a monochromatic x-ray beam and reported high-quality data on structure factors of liquids (argon and water) in a DAC. Shen *et al.*¹⁰ reported the results of structural studies of amorphous material at high pressures with the ADS technique. In this article, we describe a modified DAC suitable for structural studies of noncrystalline materials at very high pressures. A procedure for absorption correction and background subtraction is presented in detail. An analysis process is demonstrated using our data for amorphous iron collected at 67 GPa. Although the present discussion is focused on amorphous solids, it should be applicable to structural studies of liquids as well.

II. DIAMOND ANVIL CELL

A symmetric diamond anvil cell¹¹ is used. Originally designed for laser heating experiments,^{11,12} this cell has an x-ray opening of 60° (Fig. 1). It is compact, with dimensions approximately 45 mm in diameter and 35 mm in length, yet pressures in the Mbar range have been reached.^{13,14} The cell has been applied to many research areas, such as *in situ* laser heating,¹² radial diffraction,¹³ and high-resolution emission spectroscopy.¹⁵

Tungsten carbide (WC) seats are generally used as the supporting bases for the diamond anvils. In general, a conical

^{a)}Author to whom correspondence should be addressed; electronic mail: shen@cars.uchicago.edu

^{b)}Also at Department of Geophysical Sciences, University of Chicago, Chicago, IL 60637.

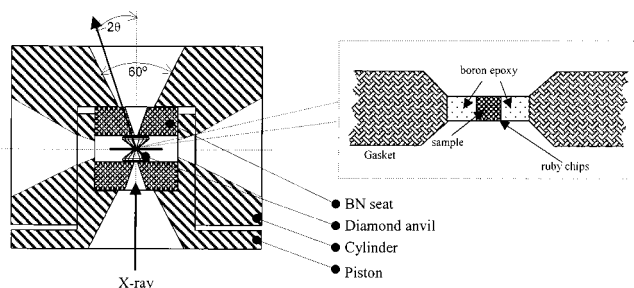


FIG. 1. Symmetrical diamond anvil cell (see Ref. 11). The BN seat is used for large x-ray scattering angle. The enlarged view is the sample configuration. A hole slightly larger than the culet is drilled and then filled with the boron epoxy. Another smaller hole is drilled at the center of the boron epoxy for sample loading. This configuration results in an increase of the sample thickness and minimum deformation of the metallic gasket hole at high pressures.

aperture is machined in the WC seat for analytical access to the sample located between the two anvil culets. The design of the conical aperture is mainly determined by two factors: the applied force needed to reach the desired pressure and the required access opening to the sample for radiation, including visible and x ray. In principle, knowing the mechanical properties of the WC seat, it is possible to predict an optimal design with the help of techniques such as finite-element modeling. In practice, we are not aware of any such simulation, and the aperture size and shape are mostly determined from experience. Typically, an aperture size at the diamond side is determined by the desired pressure range and the size of the anvil. The aperture opening angle is determined by the required visible optical access to the sample, taking into account the refractive index of diamond. For example, for a cell that can go routinely to Mbar pressures, a small hole of less than 1.2 mm is used. With a typical anvil thickness of 2.5 mm, the full visible optical opening is $\sim 70^\circ$; while the full opening for x ray is only 27° . In the normal case that the incident x ray is parallel to the loading axis, the x-ray diffraction angle (2θ) is limited to 13.5° .

To increase the opening angle, x-ray transparent materials have been introduced. Beryllium seats are widely used for single-crystal studies.¹⁶ Boron seats were used for ultrahigh-pressure single-crystal study¹⁷ and for x-ray scattering of liquids.⁹ Here, we use boron nitride (BN) as the seat material. BN is the second hardest material (next to diamond), and is x-ray transparent, with an absorption coefficient comparable to that of diamond. For example, at the energy of 37.44 keV, the absorption coefficient is $0.2139 \text{ cm}^2/\text{g}$ ($0.2157 \text{ cm}^2/\text{g}$ for diamond).¹⁸ Such BN seats are now commercially available.

A large scattering opening, and thus the momentum transfer $Q = 4\pi \sin \theta/\lambda$, is essential for structural studies of noncrystalline materials. Figure 2 shows the maximum momentum transfer as a function of the x-ray energy with various access opening angles. The typical energy range used for DAC study is also shown. In general, a maximum momentum transfer (Q_{max}) of more than 80 nm^{-1} is required to avoid introducing significant truncations effects¹⁹ on the structure of noncrystalline materials. As shown in Fig. 2, an access opening with 2θ of 13.5° (in the case of WC seats) is

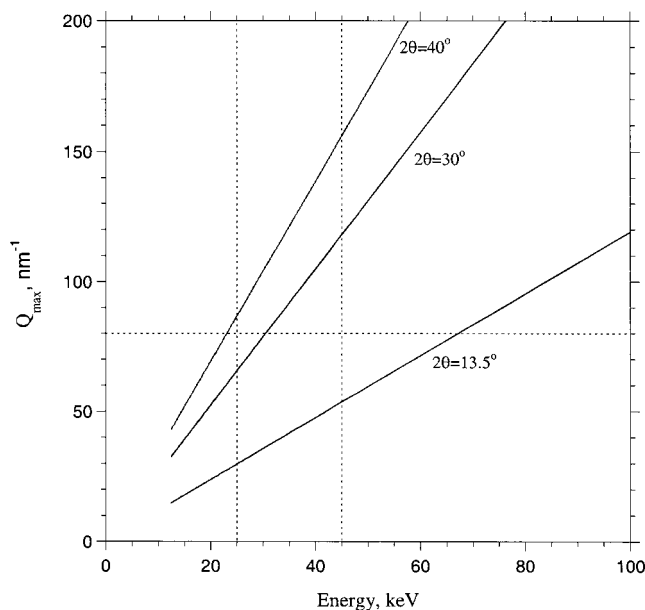


FIG. 2. Accessible momentum transfer with various scattering angles as a function of x-ray energy. X-ray energies for DAC experiments are, typically, in the range of 25–45 keV. Q_{max} larger than 80 nm^{-1} is usually required.

not large enough to have reasonable Q coverage. For an opening with 2θ of 30° (as in this study, Fig. 1), x-ray energies larger than 30 keV are required. At the energy of 37.44 keV ($\lambda = 0.3311 \text{ \AA}$), a typical energy used at the GSECARS sector for DAC experiments, Q_{max} extends to 98 nm^{-1} .

The enlarged view in Fig. 1 is the sample configuration in the DAC. The new feature introduced is the use of amorphous boron epoxy. The boron epoxy was prepared by mixing amorphous boron (Alfa) with epoxy (Epo-tek) in 4:1 ratio by weight. There are two major advantages of using boron epoxy: increased sample thickness and minimum deformation of the metallic gasket at high pressures, for a proper background reference.

In x-ray scattering experiments with the DAC, the sample signal-to-anvil-background ratio may be improved by increasing the sample thickness and/or decreasing the thickness of the diamond anvils.⁹ However, decreasing the anvil thickness is generally not favored because the achievable pressure range will then be reduced. Therefore, increasing the sample thickness with the use of boron gasket inserts is a critical factor for obtaining measurable x-ray scattering of amorphous materials at ultrahigh pressures.

The other advantage of using boron gasket inserts is in background subtraction. Because of the large scattering from diamond anvils, a measurement of the scattering from the empty cell (without the sample, but with all the rest of the parts of the DAC identical to that used for high-pressure data collection) is necessary. Among these parts, the most critical item is the metallic gasket, generally made of high-Z materials (e.g., rhenium). Since the metallic gasket hole serves as an aperture for the scattering from the first diamond, great care must be taken in collecting the background data with respect to the location, shape, and size of the "aperture." If no boron epoxy were inserted, the metallic gasket hole would inevitably deform at high pressures. Consequently, it

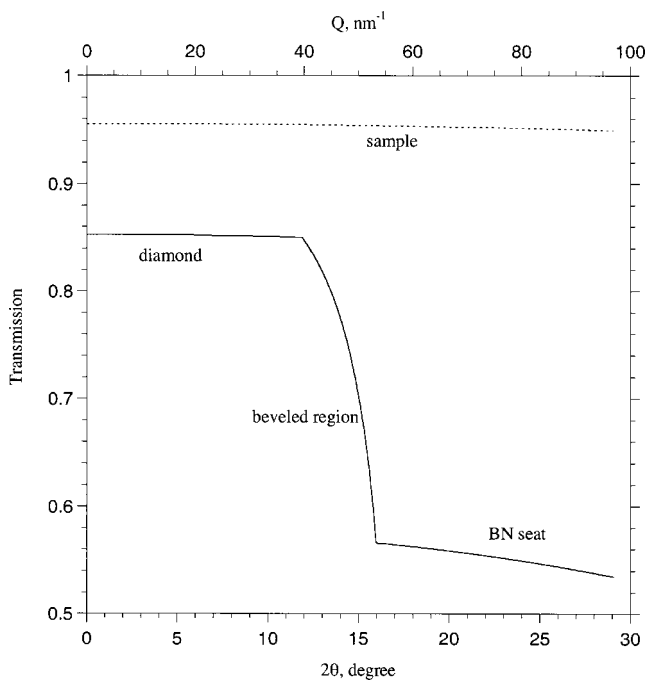


FIG. 3. Calculated transmission function from geometry of the diamond anvil and the BN seat. The sample self-absorption effect is also shown.

would be impossible to have an identical aperture for a proper reference. By introducing amorphous boron (or other x-ray transparent materials) in the gasket, as shown in the enlargement in Fig. 1, the large metallic hole outside the culet area is only weakly affected at high pressures, and the deformation should happen mainly in the boron-filled area. This results in a metallic aperture close to that used in high-pressure data collection, thus providing a good background reference.

III. DATA ANALYSIS

The observed data can be expressed by the sum of the sample scattering and the background scattering:

$$I^{\text{obs}}(Q) = a(Q)I^{\text{samp}}(Q) - bI^{\text{back}}(Q), \quad (1)$$

where $a(Q)$ is the absorption factor, which is a function of the scattering angle, and b is the background correction factor. The polarization correction was applied in the image process with the software FIT2D.²⁰ To extract the sample scattering from the observed data, $a(Q)$ and b need to be determined.

A. Absorption correction

The transmission factor $a(Q)$ is dependent on Q (or the scattering angle), and can be calculated from the cell geometry and materials involved. Since the absolute absorption is included in the normalization process, it is the Q dependence that is important. As shown in Fig. 3, the transmission can be divided into three zones. The first is the absorption of the diamond anvil; the second is the absorption of the anvil and the beveled part of the BN seat; and the third zone is the absorption of the anvil and the BN seat. The sample self-absorption is usually small for thin DAC samples ($< 50 \mu\text{m}$) at high pressures. For example, change in absorption over Q

range to 100 nm^{-1} is about 0.5% for an iron sample with a thickness of $30 \mu\text{m}$ at 37.44 keV. Therefore, the self-absorption of the sample is generally neglected.

B. Background subtraction

Proper background subtraction is a challenge in structural studies of noncrystalline materials with DAC experiments. Scattering from diamond anvils is relatively large and includes Compton scattering and thermal diffuse scattering (TDS). Occasionally, Bragg diffraction spots from diamonds may be recorded, which can be easily removed by masking the image in the integration process. Removing the Compton scattering and TDS may be made experimentally with a proper background measurement. Because TDS is strongly dependent on temperature, it is necessary to have a background measurement for each sample temperature. Two methods may be applied to obtain the background reference. One is the empty cell reference, i.e., a background scattering without the sample in the same cell with the same gasket as those used for high-pressure data collection. As mentioned above, the use of boron gasket inserts helps to preserve a gasket with a hole size and shape almost identical to those at high pressures, providing a proper reference with the empty cell method. The other method is to obtain a background reference from a corresponding crystalline sample of the noncrystalline material. This method becomes particularly practical and easy when measurements are made near freezing points crossing a melting curve.^{9,21}

Having obtained a reference background, it is found that factor b in Eq. (1) is often not unity. This could be due to variations in incident beam intensity, detector temperature, and other time-dependent factors. For the DAC shown in Fig. 1, sample scattering at 2θ angles larger than 30° is blocked by the cell body. This provides a way of determining the factor b , by constraining the sample scattering signal to be zero in this region (Fig. 4).

C. Normalization

After obtaining the sample scattering $I^{\text{samp}}(Q)$ with proper absorption and background corrections, the rest of the data analysis is similar to most noncrystalline scattering experiments. The description of the atomic distribution in noncrystalline materials usually employs the concepts of the structure factor and the pair distribution function in atomic units.

By introducing a normalization factor N , the total scattering from the sample $I^{\text{samp}}(Q)$ can be expressed in atomic units by the coherent scattering $I^{\text{coh}}(Q)$, incoherent scattering $I^{\text{incoh}}(Q)$, and the multiple scattering $I^{\text{mul}}(Q)$:¹⁹

$$NI^{\text{samp}}(Q) = I^{\text{coh}}(Q) + I^{\text{incoh}}(Q) + I^{\text{mul}}(Q). \quad (2)$$

The incoherent scattering (Compton scattering) contribution can be computed using the analytic formulas.²² Multiple scattering is generally neglected in x-ray scattering studies.¹⁹ The normalization factor N is determined by using the Krogh–Moe–Norman method.²³ By definition, the structure factor is obtained from the coherent scattering: $S(Q) \equiv I^{\text{coh}}(Q)/f^2(Q)$, where $f(Q)$ is the atomic scattering factor.

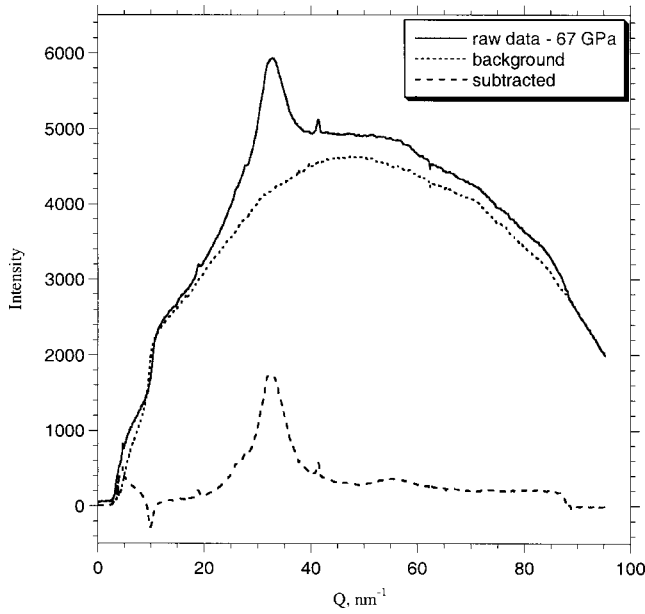


FIG. 4. Illustration of the background subtraction. An integrated pattern of x-ray scattering for amorphous iron at 67 GPa is shown, along with the empty-cell background and the background-subtracted patterns ($b = 0.715$). The oscillation in the subtracted pattern in the small- Q region arises from the position of the beamstop. A linear fit is usually applied to remove the oscillation.

The Fourier transformation of $Q[S(Q) - 1]$ is the distribution function $F(r)$ in real space:

$$F(r) \equiv 4\pi r n(r) - 4\pi r n_0$$

$$= \frac{2}{\pi} \int_0^{Q_{\max}} Q[S(Q) - 1] \sin(rQ) dQ, \quad (3)$$

where $n(r)$ is the density function of atomic number at distance r , and n_0 is the average atomic number density of the sample. From $F(r)$, the pair distribution function $g(r)$ is obtained by the definition: $g(r) \equiv n(r)/n_0$.

D. Optimization

Kaplow *et al.*²⁴ showed that $F(r)$ exhibits sharp oscillations in the small- r region arising from a normalization error. Errors in $F(r)$ from scattering factors are also apparent in the small- r region and decrease with increasing r . The oscillation in $F(r)$ in the small- r region is unphysical and can be removed by an optimization procedure. The optimization procedure should result in an improved structure factor. Several iterations may be necessary before a final $S(Q)$ and $g(r)$ is obtained.

Since the atoms do not approach each other within the atomic core diameter, $n(r)$ should be zero in this region. Therefore, from Eq. (3) we have

$$F(r) = -4\pi r n_0 \quad (r < r_{\min}), \quad (4)$$

where r_{\min} is a value close to the atomic radius. From Eq. (4), Kaplow *et al.*²⁴ and Eggert *et al.*⁹ proposed a refinement procedure for $S(Q)$ and $g(r)$. Following their approaches, we established an iterative procedure for analyzing amorphous scattering data. According to Eqs. (3) and (4), we have

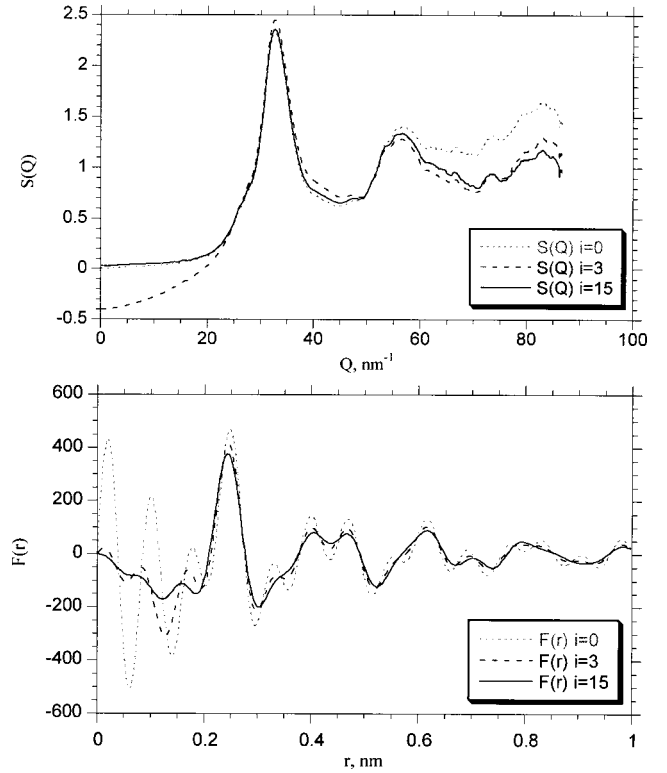


FIG. 5. Iteration evolutions of the structure factor $S_{(i)}(Q)$ (top) and the distribution function $F_{(i)}(r)$ (bottom) from the data for amorphous iron at 67 GPa. $F_{(0)}(r)$ shows oscillations in the small- r region due to errors in $S(Q)$ (see Ref. 24). Note that these oscillations converge after a few iterations. The $S(Q)$ values in the high- Q region become noisy due to the weight of atomic scattering $f(Q)$. It is shown that these $S(Q)$ values at high Q are effectively corrected with iterations.

$$F_{(i)}(r) = \frac{2}{\pi} \int_0^{Q_{\max}} Q[S_{(i)}(Q) - 1] \sin(rQ) dQ, \quad (5)$$

$$\Delta F_{(i)}(r) = F_{(i)}(r) + 4\pi r n_0 \quad (r < r_{\min}), \quad (6)$$

where i denotes the iteration number. An improved $S_{(i+1)}(Q)$ can then be obtained by applying the inverse Fourier transformation of $\Delta F_{(i)}(r)$:

$$S_{(i+1)}(Q) = S_{(i)}(Q) - \frac{1}{Q} \int_0^{r_{\min}} \Delta F_{(i)}(r) \sin(rQ) dr. \quad (7)$$

This iteration process was found to be effective in analyzing the amorphous iron sample at high pressures.¹⁰ An illustration is shown in Fig. 5 for the data at 67 GPa.

While spurious oscillations in the distribution function $F(r)$ at small values of r can be effectively removed by applying the above optimization procedure (Fig. 5), it is necessary to perform a reliability check for the corrected $S(Q)$. We make use of two criteria: (1) in the small- Q region, $\lim_{Q \rightarrow 0} S(Q) = S(0) = n_0 k_B T \beta$, where k_B is the Boltzmann constant, β is the isothermal compressibility, and T is the absolute temperature; (2) the corrected $S(Q)$ must agree with the observed data within experimental errors.

Truncation of the experimental data at Q_{\max} is a limiting factor. This is especially true for high-pressure studies because of the limited scattering angle available due to high-pressure instruments. The differences in $F(r)$ are plotted

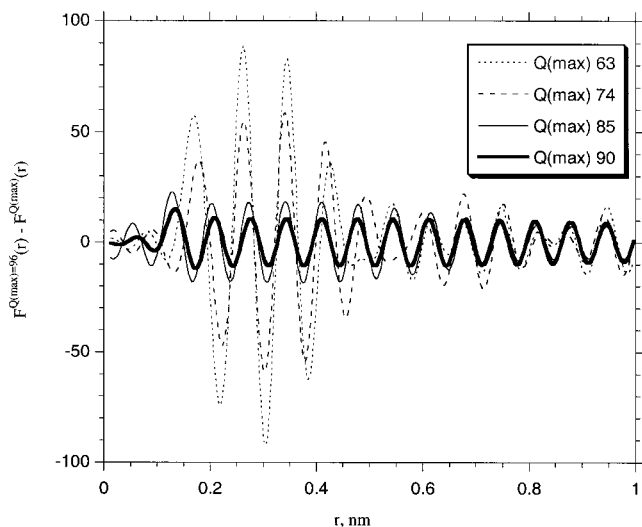


FIG. 6. Difference in $F(r)$ at various termination values from that at Q_{\max} of 95 nm^{-1} . Oscillations appear with a period of $2\pi/Q_{\max}$. Large errors arising from termination are in the vicinity of the first dominant peak.

with various Q_{\max} values (Fig. 6). Clear oscillations can be observed with an approximate period of $2\pi/Q_{\max}$. It should be noted that the greatest oscillation occurs in the vicinity of the first peak, where it holds the most critical information (Fig. 6). However, it is found that at values of Q_{\max} larger than 85 nm^{-1} errors caused by the truncating are significantly reduced. As suggested by Kaplow *et al.*,²⁴ a reliability check for the proper value of Q_{\max} should be actually the first step before all other optimization procedures. Insufficient Q range can cause inaccurate data in $F(r)$ and in the pair distribution function $g(r)$, especially in the critical region around the first peak.

An interactive data visualization (IDL) procedure was written for the above numerical analysis, a program which allows online analysis of the raw data. The initial information required are (1) the incoherent scattering $I^{\text{incoh}}(Q)$ and the atomic scattering factor $f(Q)$ of the sample, (2) the absorption function $a(Q)$ from a specific cell, and (3) the average atomic density n_0 of the sample at corresponding pressure-temperature conditions. While information (1) and (2) can be obtained or calculated, data on the atomic density n_0 are scarce, particularly at extreme conditions. Recently, using large volume presses,²⁵ densities of molten materials have been determined by the falling (or floating) ball technique. With the DAC, Eggert *et al.*⁹ estimated the density of fluids (argon and water) from the liquid structure factors measured up to 1.1 GPa. Shen *et al.*²⁶ introduced a method for density determination at high pressures in a DAC based on absorption of a monochromatic x-ray beam. It is desirable to experimentally determine n_0 at high pressures. If not available, n_0 of an amorphous material may be estimated from data at ambient pressure and then by assuming the same bulk compression as that of the corresponding crystalline phase. It is found that peak positions in both $S(Q)$ and $g(r)$ are not sensitive to the initial input values of n_0 . For example, changing n_0 by 5% leads to negligible (less than 0.02%) change in peak positions in both $S(Q)$ and $g(r)$.

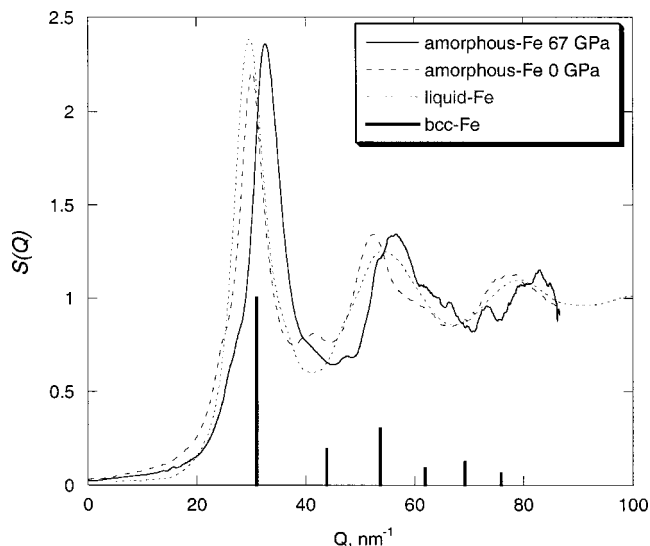


FIG. 7. Structure factor $S(Q)$ of amorphous iron at 67 GPa. Data for amorphous iron at ambient pressure and of liquid iron are shown for comparison (see Ref. 28).

E. Example: Structure of an amorphous iron at 67 GPa

Experiments on amorphous iron²⁷ were performed at the 13BM-D at the Advanced Photon Source. A monochromatic beam of 37.44 keV was used and the x-ray scattering recorded with an area detector (Bruker-2k). The structure factor and the pair distribution function of the amorphous iron sample at 67 GPa are shown in Figs. 7 and 8,²⁸ respectively, together with the data at ambient pressure and those of liquid iron for comparison. Detail structural analysis of the amorphous iron is reported elsewhere.¹⁰ The Q_{\max} value of 86.6 nm^{-1} is used to derive $g(r)$ for both 67 GPa and ambient pressure. It is found that with increasing pressure the peak height of $S(Q)$ (Fig. 7) remains essentially the same, although the peak position shifts to a higher Q value. Similar features were found in $g(r)$ in real space. The peak height in

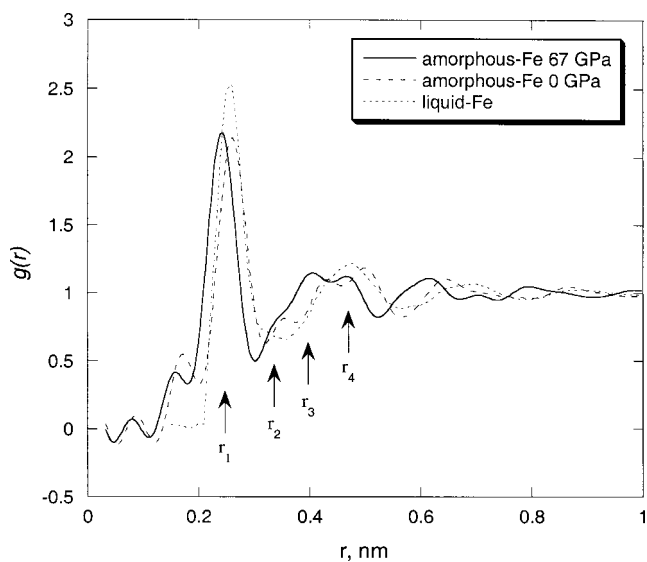


FIG. 8. Corresponding pair distribution function $g(r)$ at 67 GPa together with the data at ambient pressure and of liquid iron (see Ref. 28).

$g(r)$ does not significantly change with the increase of pressure, while the peak position shifts to smaller r values, an indication of compression.

The general structural feature of the amorphous state is similar to that of the liquid state except for a few weak peaks. In the liquid state, the amplitude of the atomic vibration is large, leading to a large uncertainty in the position of the lattice point, thus resulting in an averaged smooth distribution in both $S(Q)$ and $g(r)$ (Figs. 7 and 8). On the other hand, the small amplitude of the vibration of atoms in the amorphous state contributes to the construction of a more fixed atomic arrangement, causing some peaks in $S(Q)$ and $g(r)$ (Fig. 7).

Distance ratios of r_2/r_1 , r_3/r_1 , and r_4/r_1 in $g(r)$ (Fig. 8) at ambient pressure are found to be 1.34, 1.63, and 1.89, respectively. From the data at 67 GPa, the ratios are 1.39, 1.64, and 1.90, respectively. The weak pressure dependence of the distance ratios implies that the basic polyhedra forming the structure of the amorphous iron remain unchanged with pressure.

ACKNOWLEDGMENTS

The authors thank Nagayoshi Sata for the help in sample preparation, Ken Suslick and James Oxley for providing the amorphous sample, and Peter Eng for help during the experiment. This work is supported by NSF-EAR 0001149 and 0229987. The GSECARS sector is supported by the National Science Foundation (Earth Sciences Instrumentation and Facilities Program) and Department of Energy-Basic Energy Sciences (Geoscience Program).

¹D. Alfe, G. Kresse, and M. J. Gillan, *Phys. Rev. B* **61**, 132 (2000); V. V. Brazhkin and A. G. Lyapin, *Phys. Usp.* **43**, 493 (2000).

²N. H. March, *Liquid Metals: Concepts and Theory* (Cambridge University Press, Cambridge, New York, 1990); N. W. Ashcroft and J. Lekner, *Phys. Rev.* **145**, 83 (1965).

³P. Ascarelli, *Phys. Rev.* **173**, 2711 (1968); M. Hasegawa and M. Watabe, *J. Phys. Soc. Jpn.* **32**, 14 (1972); S. A. Trigger, V. B. Bobrov, and Yu. P. Vlasov, *Physica B* **193**, 291 (1994).

⁴M. Hasegawa and M. Watabe, *J. Phys. Soc. Jpn.* **36**, 1510 (1974).

⁵Y. Katayama, T. Mizutani, W. Utsumi, O. Shimomura, M. Yamakata, and K-i. Funakoshi, *Nature (London)* **403**, 170 (2000).

⁶W. A. Crichton, M. Mezouar, T. Grande, S. Stolen, and A. Grzechnik, *Nature (London)* **414**, 622 (2001).

⁷S. Urakawa, N. Igawa, N. Umisaki, K. Igarashi, O. Shimomura, and H. Ohno, *High Press. Res.* **14**, 375 (1996); K. Tsuji, K. Yaoita, M. Imai, O. Shimomura, and T. Kikegawa, *Rev. Sci. Instrum.* **60**, 2425 (1989); C. Meade, R. J. Hemley, and H. K. Mao, *Phys. Rev. Lett.* **69**, 1387 (1992); M. B. Kruger and C. Meade, *Phys. Rev. B* **55**, 1 (1997).

⁸K. Yaoita, Y. Katayama, K. Tsuji, T. Kikegawa, and O. Shimomura, *Rev. Sci. Instrum.* **68**, 2106 (1997); M. Mezouar, P. Faure, W. Crichton, N. Rambert, B. Sitaud, S. Bauchau, and G. Blattmann, *ibid.* **73**, 3570 (2002).

⁹J. H. Eggert, G. Weck, P. Loubeyre, and M. Mezouar, *Phys. Rev. B* **65**, 174105 (2002).

¹⁰G. Shen, M. L. Rivers, S. R. Sutton, N. Sata, V. B. Prakapenka, K. S. Suslick, and J. Oxley, *Phys. Earth Planet. Inter.* (submitted).

¹¹H. K. Mao, G. Shen, R. J. Hemley, and T. S. Duffy, in *Properties of Earth and Planetary Materials*, edited by M. H. Manghnani and T. Yagi (AGU, Washington, DC, 1998), p. 27.

¹²G. Shen, M. L. Rivers, Y. Wang, and S. R. Sutton, *Rev. Sci. Instrum.* **72**, 1273 (2001).

¹³H. K. Mao, J. Shu, G. Shen, R. J. Hemley, B. Li, and A. K. Singh, *Nature (London)* **396**, 741 (1998).

¹⁴S. H. Shim, T. S. Duffy, and G. Shen, *Science (Washington, DC, U.S.)* **293**, 2437 (2001).

¹⁵J. Badro, R. J. Hemley, H. K. Mao, V. V. Struzhkin, J. Shu, G. Shen, C. C. Kao, J. P. Rueff, and J. Hu, *Phys. Rev. Lett.* **20**, 4101 (1999); J. Badro, G. Fiquet, V. V. Struzhkin, M. Somayazulu, H. K. Mao, G. Shen, and T. Le Bihan, *ibid.* **89**, 205504 (2002).

¹⁶L. Merrill and W. A. Bassett, *Rev. Sci. Instrum.* **45**, 290 (1974); H. K. Mao and R. J. Hemley, *High Press. Res.* **14**, 257 (1996).

¹⁷P. Loubeyre, R. LeToullec, D. Hausermann, M. Hanfland, R. J. Hemley, H. K. Mao, and L. W. Finger, *Nature (London)* **383**, 702 (1996).

¹⁸M. J. Berger and J. H. Hubbell, Report No. NBSIR 87-3597 (1987).

¹⁹Y. Waseda, *The Structure of Noncrystalline Materials* (McGraw-Hill, New York, 1980).

²⁰A. P. Hammersley, S. O. Sevsson, M. Hanfland, A. N. Fitch, and D. Häusermann, *High Press. Res.* **14**, 235 (1996).

²¹G. Shen, N. Sata, N. Taberlet, M. Newville, M. L. Rivers, and S. R. Sutton, *J. Phys.: Condens. Matter* **14**, 1 (2002).

²²J. Thakkar and D. C. Chapman, *Acta Crystallogr., Sect. A: Cryst. Phys., Diffr., Theor. Gen. Crystallogr.* **A31**, 391 (1975); H. H. M. Balyuzi, *ibid.* **A31**, 600 (1975).

²³J. Krogh-Moe, *Acta Crystallogr., Sect. A: Cryst. Phys., Diffr., Theor. Gen. Crystallogr.* **9**, 951 (1956); N. Norman, *ibid.* **10**, 370 (1957).

²⁴R. Kaplow, S. L. Strong, and B. L. Averbach, *Phys. Rev.* **138**, A1336 (1965).

²⁵Y. Katayama, K. Tsuji, O. Shimomura, T. Kikegawa, M. Mezouar, D. Martinez-Garcia, J. M. Besson, D. Hausermann, and M. Hanfland, *J. Synchrotron Radiat.* **5**, 1023 (1998); C. Sanloup, F. Guyot, P. Gillet, G. Fiquet, M. Mezouar, and I. Martinez, *Geophys. Res. Lett.* **27**, 811 (2000).

²⁶G. Shen, N. Sata, M. Newville, M. L. Rivers, and S. R. Sutton, *Appl. Phys. Lett.* **81**, 1411 (2002).

²⁷K. S. Suslick, S. B. Choet, A. A. Cichowlas, and M. W. Grinstaff, *Nature (London)* **353**, 414 (1991).

²⁸Y. Waseda and K. Suzuki, *Phys. Status Solidi* **39**, 669 (1970).